

1990

A Fluid Flow and Valve Force Model for the Suction Side of a Variable Speed Heat Pump Compressor

S. D. Lewis

Tecumseh Products Research Laboratory

G. W. Gatecliff

Tecumseh Products Research Laboratory

Follow this and additional works at: <https://docs.lib.purdue.edu/icec>

Lewis, S. D. and Gatecliff, G. W., "A Fluid Flow and Valve Force Model for the Suction Side of a Variable Speed Heat Pump Compressor" (1990). *International Compressor Engineering Conference*. Paper 741.
<https://docs.lib.purdue.edu/icec/741>

This document has been made available through Purdue e-Pubs, a service of the Purdue University Libraries. Please contact epubs@purdue.edu for additional information.

Complete proceedings may be acquired in print and on CD-ROM directly from the Ray W. Herrick Laboratories at <https://engineering.purdue.edu/Herrick/Events/orderlit.html>

A FLUID FLOW AND VALVE FORCE MODEL FOR THE SUCTION SIDE OF A VARIABLE SPEED HEAT PUMP COMPRESSOR

Steven D. Lewis, Research Engineer
George W. Gatecliff, Ph.D., Chief Research Engineer

Tecumseh Products Research Laboratory
Ann Arbor, Michigan USA

ABSTRACT

A model of the time-varying fluid flow in the suction lines of a reciprocating compressor is presented. The model utilizes an impedance type solution to the linearized, one-dimensional acoustic wave equation and can be run as a part of a compressor simulation to predict compressor performance and suction valve behavior. The performance and suction valve behavior of a 2 1/2 ton compressor were predicted for several running speeds under low mass flow (heat pump) conditions. Comparisons to experimental data illustrate the validity of the approach and the improvement it provides over a constant suction plenum pressure model.

INTRODUCTION

When a reciprocating compressor is allowed to operate over a wide range of running speeds, the potential to excite resonant fluid behavior in the compressor's flow passages piping network exists, and this can have a profound effect on its performance. A two-cylinder, two and one half ton production compressor was tested on a calorimeter at five different running speeds under heat pump conditions. Measurements of the pressure pulsations indicated the existence of resonant behavior in the suction plenum. Thus, a model of the time dependent flow in the suction lines was developed in an effort to analyze this behavior, and the model is presented in this paper.

The approach to the model is very similar to the approach taken by Singh and others in a model of the flow in the discharge lines of a reciprocating compressor [1]. The model presented here is unique in the fact that it is applied to the suction side of the compressor and that it was tested at several different running speeds.

ACOUSTIC WAVE EQUATION

The linearized acoustic wave equation is used to model the pressure pulsations in the suction lines of a reciprocating compressor. Various researchers have been successful using the linearized wave equation to model refrigerant flow in a compressor for pulsation amplitudes as large as 15-20% of the mean pressure. The model presented in this paper includes the effect of viscous damping and is based on the form of the wave equation shown below [2]:

$$\partial^2 p / \partial t^2 = c^2 \partial^2 p / \partial x^2$$

Expressing the viscous damping effect in this manner assumes a circular cross section for the suction lines and a harmonic solution to the wave equation:

$$p(x,t) = P(x)e^{j\omega t} \quad 2$$

An expression for the refrigerant velocity, u , is obtained from the continuity equation

$$\partial u / \partial x = (-1/(\rho c^2))(\partial p / \partial t) \quad 3$$

where

$$u(x,t) = U(x)e^{j\omega t} \quad 4$$

The mass flow rate, $m(x,t)$, can then be written:

$$m(x,t) = M(x)e^{j\omega t} = \rho S U(x)e^{j\omega t} \quad 5$$

SOLUTION TO THE WAVE EQUATION

The harmonic solution to the acoustic wave equation is:

$$p(x,t) = (Ae^{-\gamma x} + Be^{\gamma x})e^{j\omega t} \quad 6$$

Equations 3 - 6 imply the following expression for mass flow rate

$$m(x,t) = S c' (Ae^{-\gamma x} - Be^{\gamma x})e^{j\omega t} / c^2 \quad 7$$

where the constants A and B are determined from the boundary conditions:

$$p(0,t) = P_0 e^{j\omega t} \quad 8$$

$$p(L,t) = P_L e^{j\omega t}$$

A four pole matrix which relates the pressures and mass flow rates at the two ends can be derived from the application of these boundary conditions.

$$\begin{bmatrix} P_0 \\ M_0 \end{bmatrix} = \begin{bmatrix} \cosh(\gamma L) & -j\gamma c^2 \sinh(\gamma L) / (\omega S) \\ j\omega S \sinh(\gamma L) / (\gamma c^2) & \cosh(\gamma L) \end{bmatrix} \begin{bmatrix} P_L \\ M_L \end{bmatrix} \quad 9$$

FOURIER SERIES REPRESENTATION OF PRESSURE AND MASS FLOW RATE

In reality the pressure and mass flow rates are not simple harmonic functions as implied in equations 2 and 5. They are, however, periodic where the period equals the time required for one crankshaft revolution. Thus, it is possible to represent each of these quantities as a Fourier series.

$$p(x,t) = P_0 + \sum_n P(x, n\omega_0) * \cos(n\omega_0 t + \phi(n\omega_0)) \quad 10$$

$$m(x,t) = m_0 + \sum_n M(x, n\omega_0) * \cos(n\omega_0 t + \theta(n\omega_0)) \quad 11$$

It is convenient to express the quantities in equations 10 and 11 as complex numbers where the cosine series is the real part of the complex number. Thus at point, x_i , in the pipe

$$\underline{P}_i(n\omega_0) = P(x_i, n\omega_0) e^{j\phi(n\omega_0)} \quad 12$$

$$\underline{M}_i(n\omega_0) = M(x_i, n\omega_0) e^{j\theta(n\omega_0)} \quad 13$$

It can be shown that the pressure and mass flow rate at point x_i are given by the following expressions.

$$p(x_i, t) = p_o + \int \text{Real}\{\underline{P}_i(n\omega_o)e^{j\omega t}\} \quad 14$$

$$m(x_i, t) = m_o + \int \text{Real}\{\underline{M}_i(n\omega_o)e^{j\omega t}\} \quad 15$$

If the points x_1 and x_2 are boundary points, the four pole matrix can be used to relate the complex pressures and mass flow rates at these points.

$$\begin{bmatrix} \underline{P}_i(n\omega_o) \\ \underline{M}_i(n\omega_o) \end{bmatrix} = [F(n\omega_o)] \begin{bmatrix} \underline{P}_j(n\omega_o) \\ \underline{M}_j(n\omega_o) \end{bmatrix} \quad 16$$

where $[F(n\omega_o)]$ is the four pole matrix at frequency $n\omega_o$.

APPLICATION TO A TWO-CYLINDER COMPRESSOR

The suction muffler in a two-cylinder reciprocating compressor consists of several pipes, and a four pole matrix is derived for each pipe in the suction network and for a specified number of harmonics of the fundamental running frequency. The four pole matrices are assembled to generate an overall four pole matrix of the system. An impedance matrix may be derived from the overall four pole matrix which relates the pressures and mass flow rates at the suction plenums.

$$\begin{bmatrix} \underline{P}_1(n\omega_o) \\ \underline{P}_2(n\omega_o) \end{bmatrix} = [Z(n\omega_o)] \begin{bmatrix} \underline{M}_1(n\omega_o) \\ \underline{M}_2(n\omega_o) \end{bmatrix} \quad 17$$

If the mass flow rate as a function of time is known, equations 13, 14, 15, and 17 become the model of the time dependent flow in the suction lines and provide a means for calculating pressure pulsations in the suction plenum.

SIMULATION

These concepts are incorporated into a compressor simulation which models the cylinder processes, valve dynamics and refrigerant flow through the ports. Initially, the suction muffler is modeled as a network of pipes. The impedance matrix is computed based on the geometry of these pipes and the operating conditions. The simulation predicts the mass flow rate as a function of time based on constant plenum pressure. A Fourier transform is performed on the mass flow rate curve from which the complex representation of the mass flow rate can be determined. The impedance matrix is then used according to equation 17 to compute the complex representation of the suction plenum pressure. The plenum pressure as a function of time can be calculated from equation 14, and the simulation predicts the mass flow rate as a function of time based on the updated plenum pressure. This process is repeated until the plenum pressure converges. A flow chart illustrating this procedure is given in Figure 1.

RESULTS

The fluid flow model was tested by analyzing a two-cylinder production compressor. Compressor performance was predicted for operation in the heat pump mode at several different running speeds between 60 and 120 Hz, and the results were compared to experimental data. The network used to model the suction muffler is depicted in Figure 2.

VISCOUS DAMPING FACTOR

When the simulation is run using the theory that has been described, the iterative procedure does not converge. This is because the flow model is under damped. The theory presented only accounts for viscous damping, while other forms of energy dissipation are present within the compressor. These include [3]:

- 1) Thermal conductivity boundary dissipation
- 2) Flow induced damping
- 3) Finite amplitudes
- 4) Radiation resistance

These energy dissipation mechanisms are modeled by multiplying the viscous damping term by an appropriate factor (4). Thus,

$$\alpha_t = K\alpha$$

18

and α_t is used in place of the viscous damping term, α , in the flow model.

PERFORMANCE PLOTS

Figure 3 illustrates the capacity vs. speed relationship predicted by the simulation using constant suction plenum pressure. The figure illustrates the necessity of a time-varying fluid flow model. The dip in capacity near 105 Hz is due to extraneous suction valve openings caused by pressure oscillations in the suction plenum. Thus, a simulation which uses constant suction plenum pressure can not predict these trends since it does not account for these oscillations. This phenomenon is shown in Figure 3.

Figure 4 depicts the capacity vs. speed relationship predicted by a new compressor simulation which uses the fluid model presented here and a damping correction factor of 150. The value of 150 for the damping correction factor is suggested in the literature [4], and it supplied quick, reliable convergence. The correlation between the measured and predicted results is poor, however, and the predicted capacity vs. speed relationship looks very similar to that determined by the simulation which uses constant suction plenum pressure. This result indicates that the damping correction factor is excessively large for the application being analyzed and damps out all of the plenum pressure pulsations. Thus, the plenum pressure approaches a constant value forcing the time-varying fluid flow model to behave almost identically to the constant plenum pressure model.

Figure 5 gives the capacity vs. speed relationship using a damping correction factor of 75. The simulation correctly predicts the trend in capacity as the speed varies, and the predicted results closely match the measured data at all speeds except 120 Hz. The plot of measured suction plenum pressure at 120 Hz, Figure 9, illustrates why the simulation fails at this speed. The peak-to-peak amplitude of the pulsations are roughly 40 percent of the mean plenum pressure, and linear acoustic theory is only valid when the peak-to-peak amplitudes are less than 20 percent of the mean pressure. Therefore, the flow is not governed by the linear wave equation, and an accurate determination of the plenum pressure can not be obtained by this means.

Compressor performance was predicted for running speeds of 60, 75, 90, 105, and 120 Hz. Figures 6 and 7 are representative plots of the predicted suction plenum pressure at 90 and 120 Hz respectively, and Figures 8 and 9 are the corresponding plots for the measured data. The plots indicate that the general character of the suction plenum pressure is preserved by the fluid flow model. The second harmonic is dominant in both the measured and predicted results, and the timing of the relative maxima and minima points is the same for both the measured and analytical data.

The most noticeable discrepancy between the measured and predicted suction plenum pressure is the omission of some high frequency characteristics. This is due to the fact that the effect of viscous damping increases with frequency, and it is further increased when multiplied by a correction factor. Thus, at high frequencies the damping model predicts an unrealistic amount of energy dissipation. This does not significantly affect the accuracy of the results, however, because the amplitudes of the high frequency pulsations are small. It follows that 75 is an appropriate correction factor because it provides the proper amount of damping at the second harmonic which is the dominant frequency.

CONVERGENCE

Convergence was very reliable and rapid for the lower speeds where the validity of the linear acoustic theory is not in question. It becomes less reliable and much slower at the higher frequencies where pressure pulsations are larger. Convergence also depends heavily on the presence of viscous damping

CONCLUSIONS

A time-varying fluid flow model which permits accurate analysis of the compressor operation for a wide range of speeds has been presented. The accuracy afforded by this model offers a significant improvement over that of the constant suction plenum pressure model. The energy dissipation model is critical to both convergence and accuracy, and the model becomes less accurate as the speed is increased. This is due primarily to the fact that the pulsations become too large to be modeled by linear acoustic theory. Finally, the quantity of input data required by the model is reasonable, and this feature coupled with the accurate predictions make the simulation a useful design tool although its practicality at times is limited by slow convergence.

REFERENCES

1. Singh R., Sandgren E., Ragsdell K., and Soedel W., 1976 American Society of Mechanical Engineers Winter Annual Meeting, ASME Paper No. 76-WA/FE-10, "Simulation of a Two Cylinder Compressor for Discharge Gas Oscillation Prediction."
2. Thawani, P. T., "Analytical and Experimental Investigation of the Performance of Exhaust Mufflers with Flow," Ph. D. Thesis, The University of Calgary, 1978.
3. Singh, R., "Modeling of Multicylinder Compressor Discharge System," Ph. D. Thesis, Purdue University, 1976.
4. Singh, R., and Soedel, W., 1978 Journal of Sound and Vibration, "Assessment of Fluid Induced Damping in Refrigeration Machinery Manifolds," Vol. 57, p. 449-452.

NOMENCLATURE

- $j = (-1)^{1/2}$
 r = radius of a pipe in the flow network
 S = cross-sectional area of a pipe in the flow network
 t = time
 x = the spatial coordinate
 p = mean pressure
 \dot{m}_o = mean mass flow rate
 $p = p(x,t)$ = pressure pulsation
 $P_i(n\omega_o)$ = complex pressure for the n^{th} harmonic at point x_i
 $\bar{P}_{-1}(n\omega_o)$ = complex pressure for the n^{th} harmonic at the suction plenum for cylinder 1
 $\bar{P}_{-2}(n\omega_o)$ = complex pressure for the n^{th} harmonic at the suction plenum for cylinder 2
 $\bar{M}_i(n\omega_o)$ = complex mass flow rate for the n^{th} harmonic at point x_i
 $\bar{M}_{-1}(n\omega_o)$ = complex mass flow rate for the n^{th} harmonic at the suction plenum for cylinder 1
 $\bar{M}_{-2}(n\omega_o)$ = complex mass flow rate for the n^{th} harmonic at the suction plenum for cylinder 2
 ϕ = pressure phase angle
 θ = mass flow rate phase angle
 $u = u(x,t)$ = refrigerant velocity
 μ = dynamic viscosity of refrigerant
 ρ = density of refrigerant
 c = speed of sound
 $\alpha = \text{viscous damping term} = (\mu\omega/(2\rho c^2 r^2))^{1/2}$
 α_t = damping factor to include all forms of energy dissipation
 K = correction factor to be applied to the viscous damping
 ω = circular frequency (rad/sec)
 ω_o = fundamental circular frequency (rad/sec)
 n = n^{th} harmonic of the fundamental frequency
 k = wave number = ω/c
 k' = complex wave number = $k - j\alpha$
 c' = ω/k'
 $y = jk'$

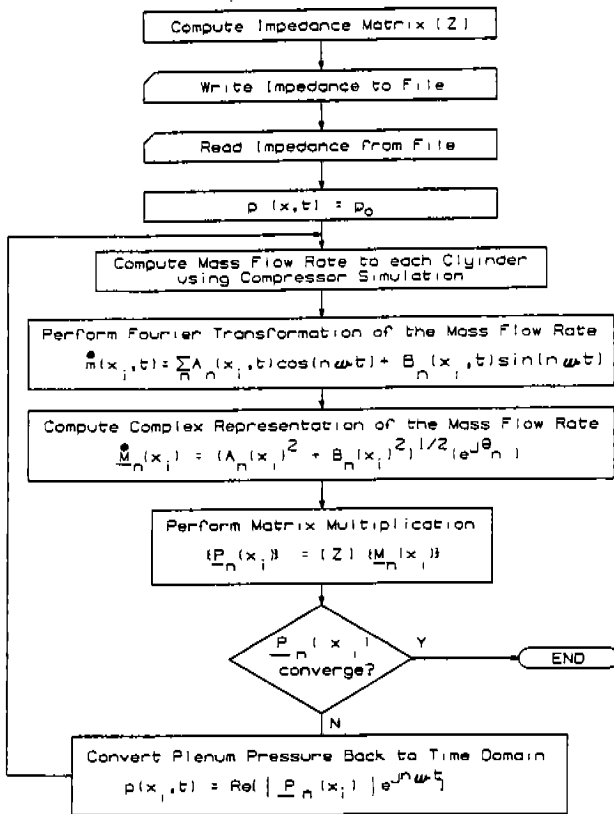


Figure 1. Flow Chart for Compressor Simulation

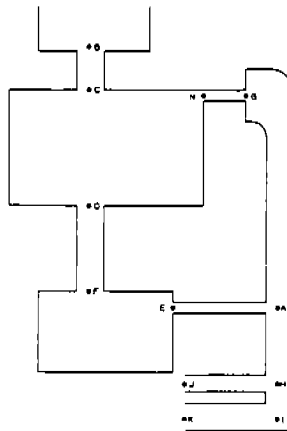


Figure 2. Schematic of Suction Muffler

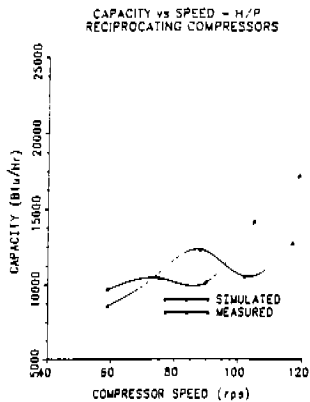


Figure 3. Predicted Heating Capacity for Time Independent Fluid Model

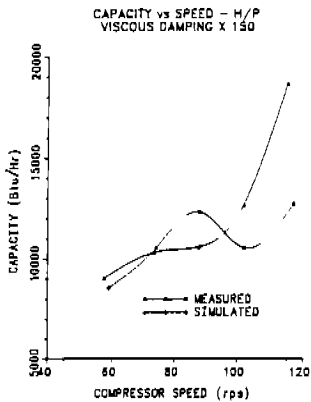


Figure 4. Predicted Heating Capacity for Time Dependent Fluid Model; K=150

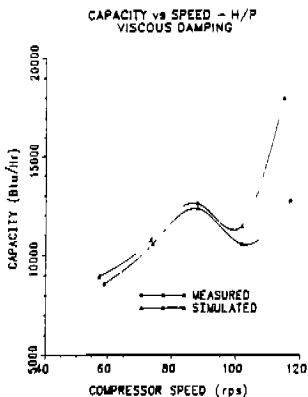


Figure 5. Predicted Heating Capacity for Time Dependent Fluid Model; K=75

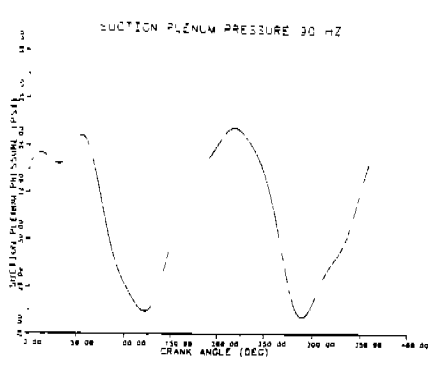


Figure 6. Predicted Suction Plenum Pressure at 90 Hz; K=75

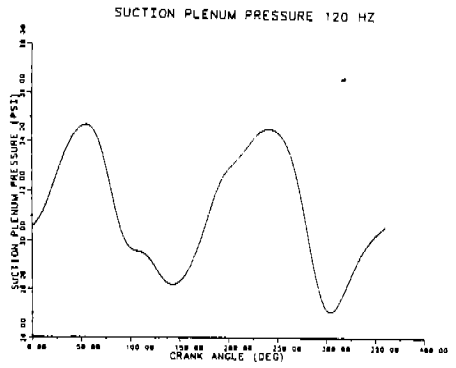


Figure 7. Predicted Suction Plenum Pressure at 120 Hz; K=75

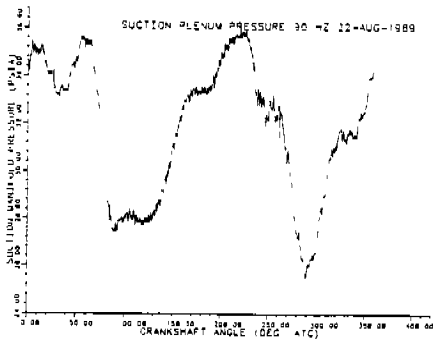


Figure 8. Measured Suction Plenum Pressure at 90 Hz

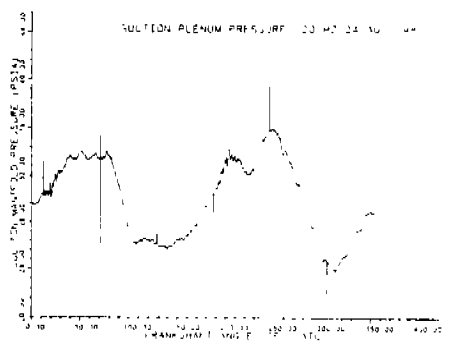


Figure 9. Measured Suction Plenum Pressure at 120 Hz